9. K. Sieh, *Philos. Trans. R. Soc. London Ser. A* **364**, 1947 (2006).
10. K. Sieh, paper presented at the First International Conference of Aceh and Indian Ocean Studies, Banda Aceh, Indonesia, 24 to 26 February 2007.
11. K. Sieh, *J. Earthquake Tsunami* **1**, 1 (2007).
12. O. Konca *et al.*, *Nature* **456**, 631 (2008).
13. J. Zachariasen, K. Sieh, F. W. Taylor, R. L. Edwards, W. S. Hantoro, *J. Geophys. Res.* **104**, 895 (1999).
14. J. Zachariasen, K. Sieh, F. W. Taylor, W. S. Hantoro, *Bull. Seismol. Soc. Am.* **90**, 897 (2000).
15. D. H. Natawidjaja *et al.*, *J. Geophys. Res.* **109**, B04306 (2004).
16. D. R. Stoddart, T. P. Scoffin, *Atoll Res. Bull.* **224**, 1 (1979).
17. C. Darwin, *The Structure and Distribution of Coral Reefs* (Smith, Elder and Co., London, 1842).
18. R. L. Edwards, F. W. Taylor, G. J. Wasserburg, *Earth Planet. Sci. Lett.* **90**, 371 (1988).
19. C.-C. Shen *et al.*, *Geochim. Cosmochim. Acta* **72**, 4201 (2008).
20. C.-C. Shen *et al.*, *Chem. Geol.* **185**, 165 (2002).
21. We use the terms "submergence" and "emergence" throughout to refer to changes with respect to a sea-level datum. We use "subsidence" and "uplift" in reference to other geodetic data and when inferring vertical tectonic motions.
22. K. Sieh, *Nature* **434**, 573 (2005).
23. Y.-J. Hsu *et al.*, *Science* **312**, 1921 (2006).
24. K. Sieh, M. Stuiver, D. Brillinger, *J. Geophys. Res.* **94**, 603 (1989).
25. G. Carver *et al.*, *Bull. Seismol. Soc. Am.* **94**, S58 (2004).
26. J. C. Borrero, K. Sieh, M. Chlieh, C. E. Synolakis, *Proc. Natl. Acad. Sci. U.S.A.* **103**, 19673 (2006).

27. This work has been supported by NSF grants EAR-9628301, 9804732, 9903301, 0208508, 0530899, 0538333, and 0809223 (to K.S.) and EAR-0207686 and 0537973 (to R.L.E.); by National Science Council grants 94-2116-M002-012 and 95&96-2752-M002-012-PAE (to C.-C.S.); by LIPI (Indonesian Institute of Science) and RUTI (International Joint Research Program of the Indonesian Ministry of Research and Technology); and by the Gordon and Betty Moore Foundation. This is Caltech Tectonics Observatory contribution number 86 and Earth Observatory of Singapore contribution number 1.

Supporting Online Material

www.sciencemag.org/cgi/content/full/322/5908/1674/DC1
SOM Text
Figs. S1 to S44
Tables S1 to S4
References

22 July 2008; accepted 8 October 2008
10.1126/science.1163589

Shock Metamorphism of Bosumtwi Impact Crater Rocks, Shock Attenuation, and Uplift Formation

Ludovic Ferrière,[1] Christian Koeberl,[1]* Boris A. Ivanov,[2] Wolf Uwe Reimold[3]

Shock wave attenuation rate and formation of central uplifts are not precisely constrained for moderately sized complex impact structures. The distribution of shock metamorphism in drilled basement rocks from the 10.5-kilometer-diameter Bosumtwi crater, and results of numerical modeling of inelastic rock deformation and modification processes during uplift, constrained with petrographic data, allowed reconstruction of the pre-impact position of the drilled rocks and revealed a shock attenuation by ~5 gigapascals in the uppermost 200 meters of the central uplift. The proportion of shocked quartz grains and the average number of planar deformation feature sets per grain provide a sensitive indication of minor changes in shock pressure. The results further imply that for moderately sized craters the rise of the central uplift is dominated by brittle failure.

During the contact and compression phase of hypervelocity impact, a spherical shock wave is generated, propagates through the target rocks (*1*), and is attenuated rapidly with increasing distance. Consequently, a variety of shock effects are produced in rock-forming minerals, including formation of planar deformation features (PDFs) and high-pressure phases. The relative spatial distribution of these shock transformations and deformations formed at different pressures and temperatures [e.g., (*2*, *3*)] in autochthonous rocks, at the scale of the impact structure, can be used to estimate maximum shock pressures and, consequently, the rate of shock attenuation. However, many parameters—such as rock type as well as lithological contrasts, texture, fabric, grain size, preshock orientation of grains, porosity, and volatile content—influence the shock levels attained locally. Furthermore, and typical in the case of complex impact structures (i.e., craters with diameters ≥2 to 4 km on Earth) (*4*), the original position and distribution of the shocked rocks is modified when, because of gravitational instability of the transient cavity rim, rebound of the crater floor leads to formation of a central uplift. Redistribution of rock is also associated with the collapse of the initially oversteepened central uplift (*5*).

There have been several efforts to estimate shock wave decay, mainly from nuclear and explosion crater studies or by numerical modeling [e.g., (*6*–*8*)]. Few studies have tried to quantify shock pressure distribution in simple (*9*) and complex impact structures (*9*–*16*) [see supporting

[1]Department of Lithospheric Research, University of Vienna, Althanstrasse 14, A-1090 Vienna, Austria. [2]Institute for Dynamics of Geospheres, Russian Academy of Sciences, Leninsky Prospect 38-1, 119334 Moscow, Russia. [3]Museum of Natural History (Mineralogy), Humboldt University, Invalidenstrasse 43, D-10115 Berlin, Germany.

*To whom correspondence should be addressed. E-mail: christian.koeberl@univie.ac.at

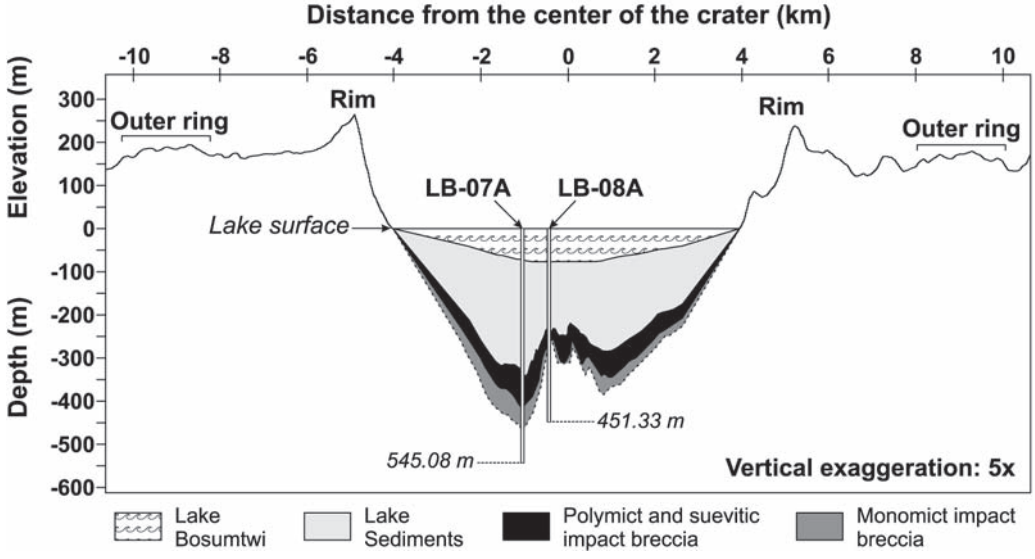

Fig. 1. Cross section of the Bosumtwi impact structure, based on Shuttle Radar Topography Mission (SRTM) data for the regional topography of the exposed portion of the crater (profile from west to east) and on a northwest-southeast seismic reflection profile (*21*) across the central crater. Location of boreholes LB-07A and LB-08A are given. The volume of lake sediments is based on seismic reflection data. The distribution of polymict and suevitic impact breccia and monomict impact breccia is based on observations from cores LB-07A and LB-08A (*19*, *20*), as well as interpretations of seismic reflection data. Depths and elevations are relative to lake level. SRTM data were available online (www2.jpl.nasa.gov/srtm/; accessed 3 March 2008).

online material (SOM text)] by using the frequency of shock-induced deformations in quartz grains from samples taken along profiles across the erosion surface of an impact structure. Only three investigations have explored the relative vertical decay of recorded shock pressure in complex impact structures, two for the ~40-km-diameter Puchezh-Katunki impact structure (*13*, *15*) and another for the ~65-km-diameter Kara crater (*11*).

We characterized the shock wave attenuation in the uppermost part of the central uplift of the Bosumtwi impact structure, a moderately sized (10.5-km diameter) and well-preserved complex impact structure [e.g., (*17*)], and attempted to reconstruct the original position of the sampled section in the target before crater modification. This is possible by combining petrographic investigations (at the microscale) with modeling of inelastic rock deformation (at the mesoscale) and modification processes during uplift (at the megascale). This approach allows us to constrain shock wave attenuation and rock deformation during central uplift formation.

We studied drill core samples from the central part of the structure retrieved in the 2004 International Continental Scientific Drilling Program (ICDP) Bosumtwi drilling project (*18*–*20*) (SOM text). The central uplift extends ~130 m above the crater moat, is ~1.9 km wide (*21*), and is composed of metasedimentary rocks [mostly metagraywacke (MGW) and shale] (*19*). Two cores were retrieved by the ICDP project: core LB-08A from the outer flank of the central uplift and core LB-07A from the deep crater moat (Fig. 1 and SOM text).

To derive the distribution of shock metamorphic effects with depth, we studied 18 MGW samples from 271.4- to 451.2-m depth in core LB-08A (Fig. 1), recording modal analysis and shock deformation properties of 8991 quartz grains (*22*) (tables S1 and S2). We determined 1056 crystallographic orientations of sets of PDFs in 602 quartz grains (table S3) because predominance of specific orientations of PDFs in quartz has long been considered to indicate different shock pressures [e.g., (*23*)].

The abundance of shocked quartz grains (i.e., quartz grains with planar fractures and/or PDFs) decreases with increasing depth (for PDFs, compare with Fig. 2). We interpret this decrease to reflect the variation of shock pressure in the uppermost part of the central uplift. Similarly, the average number of PDF sets per quartz grain (*N*) decreases steadily with depth, from ~2.1 at 271-m depth to ~1.6 at 442 m (Fig. 3). We interpret the decrease of *N* as evidence of the shock pressure attenuation with distance from shock wave origin.

No clear change was evident over this interval in the relative frequencies of the main crystallographic orientations of PDF sets in quartz grains with increasing depth (Fig. 2 and table S3). Most of the poles to the PDF planes correspond to the $\omega\{10\bar{1}3\}$ orientation, and only a few, typically less than 5 relative-percent (rel%) of the orientation data obtained per section, correspond to basal [i.e., parallel to (0001)] planes. Only two samples, KR8-85 and KR8-89, from 390- to 400-m depth, show a higher proportion of basal PDF, at about 27 and 19 rel%, respectively (table S3). These two MGW samples originated just below a 10-m-thick layer of comparatively fine-grained metasedimentary rocks (phyllite and slate; Fig. 2); thus, it is possible that shock wave interference at the transition from metapelite to MGW resulted in the local formation of a larger proportion of basal PDFs [basal PDFs are formed at lower pressures (from 8 to 10 GPa) than $\omega\{10\bar{1}3\}$ orientations (>10 GPa); e.g., (*2*)]. However, about 50% of the basal PDFs measured in these two samples occur in association with $\omega\{10\bar{1}3\}$ PDF (i.e., dual sets of PDFs in the same quartz grain), which indicates relatively high shock pressures. Thus, minor variations of the relative proportions of crystallographic orientations of PDF sets in quartz grains with depth cannot be used to quantify the slight attenuation of the shock pressure along the ~200-m-long bedrock section investigated here. Because the relative proportion of shocked quartz grains, as well as the number of PDF sets per quartz grain, steadily decrease with depth (Figs. 2 and 3), we infer that the shock wave was attenuated but not by much.

On the basis of the relative abundances of quartz grains with PDFs, the presence of multiple sets of PDFs in quartz grains (up to four sets), and the occurrence of various PDF set orientations, we estimate that the studied section experienced peak shock pressures of up to ~25 to 30 GPa [e.g., (*2*, *24*–*25*)]. The upper limit of peak shock pressure (i.e., 30 GPa) is further constrained by the lack of isotropization of the quartz grains, which typically begins at this shock pressure [e.g., (*2*)]. The estimated pressure range is much too low for either

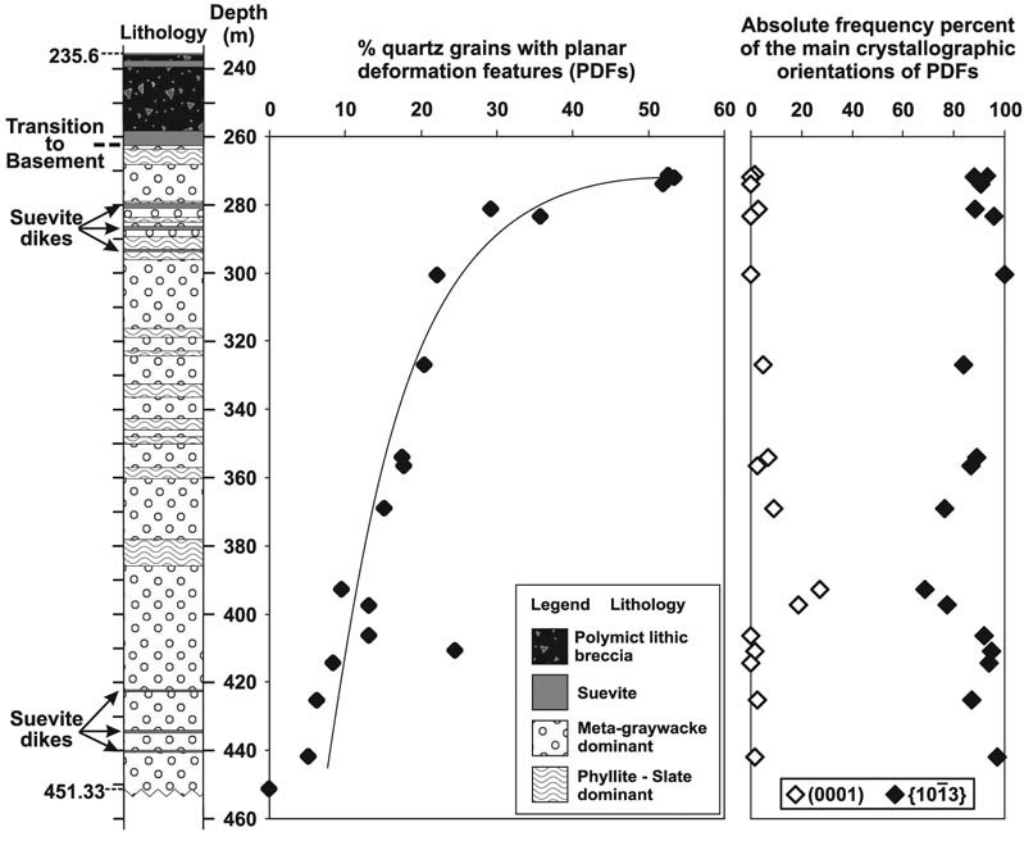

Fig. 2. Simplified lithostratigraphic column for drill core LB-08A [after (*19*)] and PDF data for 18 MGW samples from the basement section. The abundance of quartz grains with PDFs relative to the total number of quartz grains is shown (left, solid diamond) and, on the right, the absolute frequency percent of the two main PDF crystallographic orientations (open diamond symbols for basal PDF and solid diamonds for $\omega\{10\bar{1}3\}$ crystallographic orientation data) in quartz grains, as measured on a universal stage.

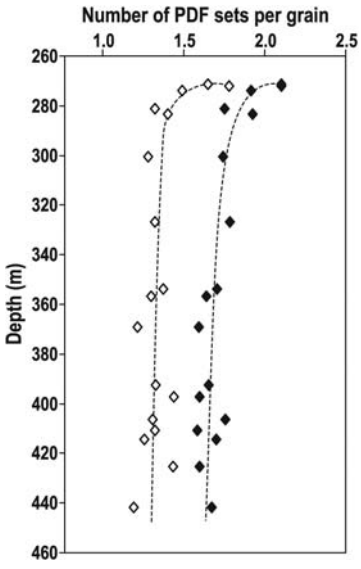

Fig. 3. Average number of PDF sets per host quartz grain (*N*) in MGW samples from the uppermost ~200 m of basement drilled in the central uplift of the Bosumtwi impact structure. For both methods, that is, with use of a petrographic microscope (under horizontal stage examination; open diamonds) and with the U stage (solid diamonds), *N* values follow the same trend of decreasing abundance of PDF sets per grain with increasing depth.

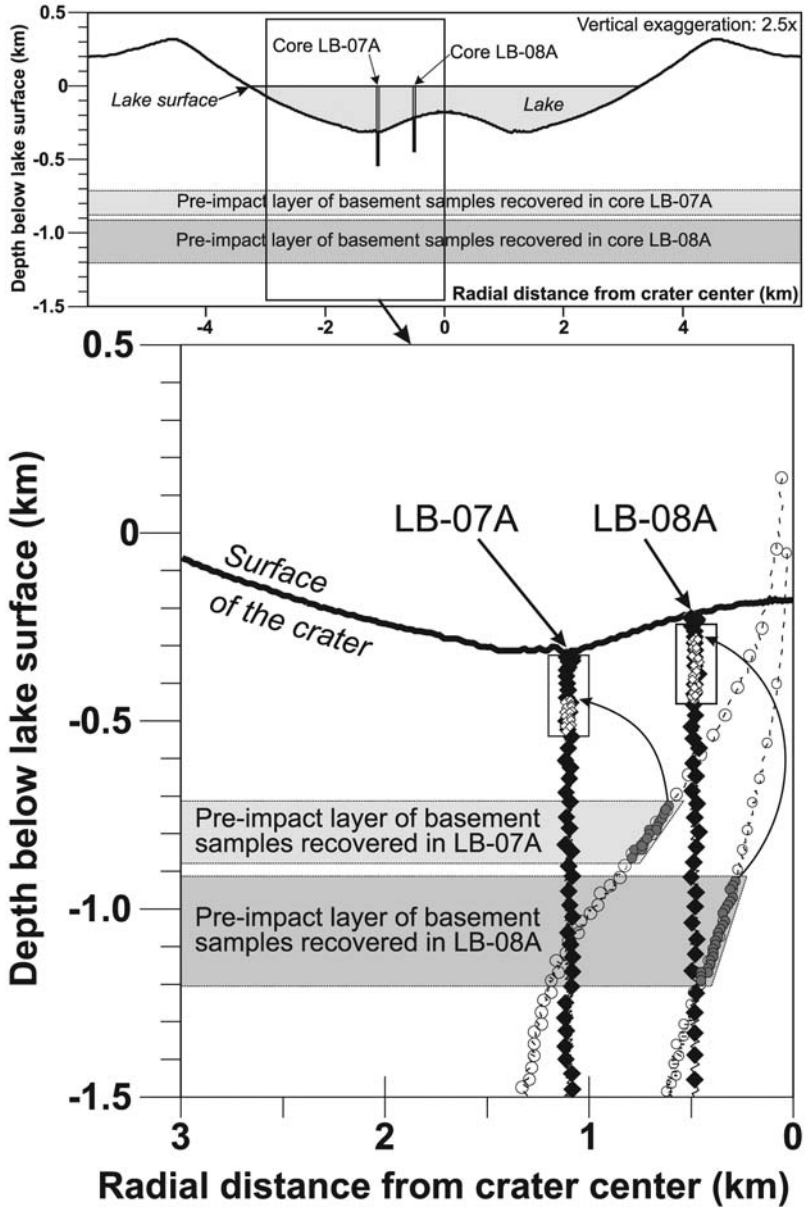

Fig. 4. Calculated crater profile with enlarged inner part showing initial and final positions of rocks recovered in drill cores LB-07A (from the crater moat) and LB-08A (from the outer flank of the central uplift). Solid diamonds show final positions of tracers (0.48- and 1.1-km radial distance from crater center), whereas open circles indicate their initial positions in the preimpact target stratigraphy. Gray dots and open diamonds show, respectively, the initial and the final positions of basement samples (i.e., investigated MGW samples in core LB-08A) recovered in drill cores. Solid diamonds above open diamonds represent the modeled impact breccia. Locations of drill cores are indicated by large open rectangles. Model run with ANEOS (analytical equation of state) granite (*28*), an impact velocity of 20 km^{-1}, and a residual friction (μ) of 0.4. For comparison of the calculated and the actual cross sections of the Bosumtwi crater, see fig. S3.

partial or total shock melting of the whole rock, which is in agreement with macroscopic and microscopic observations on these metasedimentary rocks that have preserved their preimpact texture (*19*) (SOM text). Thus, the rise of the central uplift was not facilitated by shock-induced plasticity, and brittle failure was dominant. This finding is also supported by the presence of abundant faults in the central uplift, as indicated by reflection seismic data (*21*).

To further evaluate the apparent shock attenuation, we calculated the expected shock pressure attenuation and reconstructed the preimpact position of the investigated section of the central uplift by numerical modeling, by using a variant of the SALEB numerical code (*26*) (SOM text). To model the crater and central uplift properly, we did a direct parametric fit of our model to the observed crater geometry without usage of scaling relations for the crater size (SOM text and fig. S3). After modeling, tracers in the vicinity of the exact location of the two drill holes were identified (allowing the tracking of their initial positions), and lastly the position of the top of the "model core" was defined by the maximum recorded shock pressure of 30 GPa (based on our petrographic investigations). Then, the initial position of these tracers was plotted (Fig. 4). Our calculations show that, despite quite similar present-day depths, the initial depth of rocks in the crater moat (core LB-07A) was above that of the rocks in the central uplift corehole (Fig. 4). This specific displacement of the target rocks during crater modification is interesting because it indicates that rocks occurring in the outer flank of the central uplift were originally more deeply buried than the basement rocks drilled below the deep crater moat and, thus, were subjected to somewhat lower shock pressures. Thus, before estimating shock attenuation in complex impact structures, it is important to consider the differential movements of the target rocks, which cause changes in the spherical shock-attenuation scheme. The numerical model (Fig. 4 and SOM text) indicates that the samples investigated in core LB-08A have been uplifted by about 1.2 to 1.5 km. By using the relationship $SU = 0.086D^{1.03}$ (*27*) (where D is the crater diameter), we estimated the amount of structural uplift (*SU*) for the Bosumtwi central uplift at about 1 km, in good agreement with the modeling result.

Taking into account the uplift of target rocks, the calculated apparent shock attenuation along the about-200 m of investigated core is ~5 to 10 GPa (fig. S4). On the basis of the general absence of

changes in the statistics of PDF orientations, a maximum shock attenuation of 5 GPa seems to be the more realistic value.

The percentage of shocked quartz grains and the number of PDF sets per grain are more sensitive indicators of minor changes in shock pressure than pure PDF orientation statistics. The combination of detailed petrographic investigation and numerical modeling indicates that both of these approaches are essential to reconstruct the preimpact position of rocks and to characterize properly the shock pressure distribution at the scale of an impact structure. Our observations suggest that, in the case of the 10.5-km-diameter Bosumtwi impact structure, the uppermost rocks of the central uplift experienced shock pressures below 30 GPa, whereas pressures up to 40 to 45 GPa were recorded for the about-four-times-larger Puchezh-Katunki impact structure (*15*). Shock attenuation in the uppermost part of a central uplift has been, for the first time, constrained by detailed shock degree profiling at the microscale. Numerical modeling of this section of the central uplift has then established where this section of the central uplift was located before uplift formation, which was only possible once the shock regime had been established by micropetrography. The results imply that, for moderately sized impact craters, the rise of the central uplift is dominated by brittle failure, whereas in the case of larger impact structures, and also depending on rock proprieties, the uplifted, relatively stronger shocked rocks may behave in a more ductile manner.

References and Notes

1. D. Stöffler, *Fortschr. Mineral.* **49**, 50 (1972).
2. D. Stöffler, F. Langenhorst, *Meteorit. Planet. Sci.* **29**, 155 (1994).
3. R. A. F. Grieve, F. Langenhorst, D. Stöffler, *Meteorit. Planet. Sci.* **31**, 6 (1996).
4. R. A. F. Grieve, *Annu. Rev. Earth Planet. Sci.* **15**, 245 (1987).
5. H. J. Melosh, *Impact Cratering: A Geological Process* (Oxford Univ. Press, New York, 1989).
6. J. T. Cherry, F. L. Petersen, in *Peaceful Nuclear Explosions* (International Atomic Energy Agency, Vienna, 1970), pp. 241–325.
7. T. J. Ahrens, J. D. O'Keefe, in *Impact and Explosion Cratering*, D. J. Roddy, R. O. Pepin, R. B. Merrill, Eds. (Pergamon, New York, 1977), pp. 639–656.
8. N. K. Mitani, *J. Geophys. Res.* **108**, 5003 (2003).
9. P. B. Robertson, R. A. F. Grieve, in *Impact and Explosion Cratering*, D. J. Roddy, R. O. Pepin, R. B. Merrill, Eds. (Pergamon, New York, 1977), pp. 687–702.
10. R. A. F. Grieve, P. B. Robertson, *Contrib. Mineral. Petrol.* **58**, 37 (1976).
11. L. V. Sazonova, N. N. Karotaeve, G. Y. Ponomarev, A. I. Dabizha, in *Impactites*, A. A. Marakushev, Ed. (Moscow State Univ., Moscow, 1981), pp. 93–133.
12. R. A. F. Grieve, J. M. Coderre, P. B. Robertson, J. Alexopoulos, *Tectonophysics* **171**, 185 (1990).
13. V. I. Fel'dman, L. V. Sazonova, S. I. Kotel'nikov, *Dokl. Akad. Nauk SSSR* **349**, 658 (1996).
14. B. O. Dressler, V. L. Sharpton, B. C. Schuraytz, *Contrib. Mineral. Petrol.* **130**, 275 (1998).
15. V. L. Masaitis, L. A. Pevzner, *Deep Drilling in the Impact Structure: Puchezh-Katunki, Russia* (VSEGEI, St. Petersburg, 1999).
16. R. L. Gibson, W. U. Reimold, *Geol. Soc. Am. Spec. Pap.* **384**, 329 (1996).
17. C. Koeberl, W. U. Reimold, *Yearb. Austrian Geol. Surv.* **145**, 31 (2005).
18. C. Koeberl *et al.*, *Meteorit. Planet. Sci.* **42**, 483 (2007).
19. L. Ferrière, C. Koeberl, W. U. Reimold, *Meteorit. Planet. Sci.* **42**, 611 (2007).
20. L. Coney, R. L. Gibson, W. U. Reimold, C. Koeberl, *Meteorit. Planet. Sci.* **42**, 569 (2007).
21. C. A. Scholz *et al.*, *Geology* **30**, 939 (2002).
22. Materials and methods are available as supporting material on *Science* Online.
23. F. Hörz, in *Shock Metamorphism of Natural Materials*, B. M. French, N. M. Short, Eds. (Mono, Baltimore, 1968), pp. 243–253.
24. A. R. Huffman, W. U. Reimold, *Tectonophysics* **256**, 165 (1996).
25. B. M. French, *Traces of Catastrophe: A Handbook of Shock-Metamorphic Effects in Terrestrial Meteorite Impact Structures* [LPI Contribution No. 954, Lunar and Planetary Institute (LPI), Houston, TX, 1998].
26. B. Ivanov, *Sol. Syst. Res.* **39**, 381 (2005).
27. M. J. Cintala, R. A. F. Grieve, *Meteorit. Planet. Sci.* **33**, 889 (1998).
28. E. Pierazzo, A. M. Vickery, H. J. Melosh, *Icarus* **127**, 408 (1997).

29. Drilling was funded by ICDP, NSF, the Austrian Fonds zur Förderung der wissenschaftlichen Forschung (FWF), the Canadian Natural Sciences and Engineering Research Council, and the Austrian Academy of Sciences. We thank DOSECC (Drilling, Observation and Sampling of the Earth's Continental Crust) for the drilling operations. This work was supported by the Austrian FWF (grants P17194-N10 and P18862-N10) and the Austrian Academy of Sciences. B.A.I. was supported by the Russian Foundation for Basic Science (RFBR grant 08-05-00908-a), and W.U.R.'s research is supported by the German Science Foundation (Deutsche Forschungsgemeinschaft) and Humboldt University of Berlin.

Supporting Online Material

www.sciencemag.org/cgi/content/full/322/5908/1678/DC1
Materials and Methods
SOM Text
Figs. S1 to S4
Tables S1 to S4
References

23 September 2008; accepted 10 November 2008
10.1126/science.1166283

The Spreading of Disorder

Kees Keizer,* Siegwart Lindenberg, Linda Steg

Imagine that the neighborhood you are living in is covered with graffiti, litter, and unreturned shopping carts. Would this reality cause you to litter more, trespass, or even steal? A thesis known as the broken windows theory suggests that signs of disorderly and petty criminal behavior trigger more disorderly and petty criminal behavior, thus causing the behavior to spread. This may cause neighborhoods to decay and the quality of life of its inhabitants to deteriorate. For a city government, this may be a vital policy issue. But does disorder really spread in neighborhoods? So far there has not been strong empirical support, and it is not clear what constitutes disorder and what may make it spread. We generated hypotheses about the spread of disorder and tested them in six field experiments. We found that, when people observe that others violated a certain social norm or legitimate rule, they are more likely to violate other norms or rules, which causes disorder to spread.

In the mid-1990s, the mayor of New York and his police commissioner adopted a "Quality of life campaign." Attention was focused on fighting signs of disorder and petty crime. Graffiti was removed, streets were swept, and signs of vandalism were cleared. This initiative was based on the broken windows theory (BWT) of Wilson and Kelling (*1*). The BWT suggests that signs of disorder like broken windows, litter, and graffiti induce other (types of) disorder and petty crime (*2*). It was thought that removing these signs of disorder would take away an important trigger of disorderly and petty criminal behavior. After the introduction of the campaign, petty crime rates in New York dropped. Since then, approaches based on the BWT have become popular and have been adopted worldwide (e.g., in various cities in the United States, Great Britain, Netherlands, Indonesia, and South Africa).

BWT may be very popular, but it is also highly controversial. So far, it lacks empirical support, and it fails to specify what constitutes disorder. Studies aimed to test the BWT (*3*–*6*) have provided mixed results at best. The National Research Council (NRC) concluded that the research did not provide strong support for the BWT (*7*). There is also little evidence that broken window policing contributed to the sharp decrease in petty crime in New York (*8*–*10*). Moreover, to our knowledge, research on the BWT has so far been correlational, so conclusions about causality are shaky (*6*, *8*). The BWT suggests that a setting with disorder triggers disorderly and petty criminal behavior, but it might be the other way around or both may be caused by a third variable. Furthermore, the BWT gives no insight into what is and what is not a condition of disorder that will spread. Because the BWT forms the backbone of many cities' defense against the growing threat of disorder and petty crime, these shortcomings need to be addressed.

In the present study, we conducted six field experiments that address these issues. Our first step was to conceptualize a disorderly setting in such a way that we can link it to a process of spreading norm violations. Social norms refer either to the perception of common (dis)approval of a particular kind of behavior (injunctive norm) or to a particular behavior common in a setting (descriptive norm) (*11*–*16*). Injunctive norms affect behavior because they provide information about which behavior is most appropriate in a

Faculty of Behavioral and Social Sciences, University of Groningen, 9712 TS Groningen, Netherlands.

*To whom correspondence should be addressed. E-mail: K.E.Keizer@rug.nl